Phys Chem Minerals (2006) 33: 235–242
DOI 10.1007/s00269-006-0075-0

ORIGINAL PAPER

G. Diego Gatta · F. Nestola · T. Boffa Ballaran

Elastic behaviour and structural evolution of topaz at high pressure

Received: 12 September 2005 / Accepted: 9 February 2006 / Published online: 16 March 2006

Abstract The elastic behaviour and the high-pressure structural evolution of a natural topaz, $Al_{2.00}Si_{1.05}O_{4.00}(OH_{0.26}F_{1.75})$, have been investigated by means of in situ single-crystal X-ray diffraction up to 10.55(5) GPa. No phase transition has been observed within the pressure range investigated. Unit-cell volume data were fitted with a third-order Birch-Murnaghan Equation of State (III-BM-EoS). The III-BM-EoS parameters, simultaneously refined using the data weighted by the uncertainties in P and V, are: $V_0 = 345.57(7)$ Å^3, $K_{T0} = 164(2)$ GPa and $K' = 2.9(4)$. The axial-EoS parameters are: $a_0 = 4.6634(3)$ Å, $K_{T0}(a) = 152(2)$ GPa, $K'(a) = 2.8(4)$ for the a-axis; $b_0 = 8.8349(5)$ Å, $K_{T0}(b) = 224(3)$ GPa, $K'(b) = 2.6(6)$ for the b-axis; $c_0 = 8.3875(7)$ Å, $K_{T0}(c) = 137(2)$ GPa, $K'(c) = 2.9(4)$ for the c-axis. The magnitude and the orientation of the principal Lagrangian unit-strain ellipsoid were determined. At $P-P_0 = 10.55$ GPa, the ratios $\varepsilon_1:\varepsilon_2:\varepsilon_3$ are 1.00:1.42:1.56 (with $\varepsilon_1 || b$, $\varepsilon_2 || a$, $\varepsilon_3 || c$ and $|\varepsilon_3| > |\varepsilon_2| > |\varepsilon_1|$). Four structural refinements, performed at 0.0001, 3.14(5), 5.79(5) and 8.39(5) GPa describe the structural evolution in terms of polyhedral distortions.

Keywords Topaz · High-pressure · Single crystal X-ray diffraction · Compressibility · Structural evolution

G. D. Gatta (✉)
Dip. Scienze della Terra, Sez. Mineralogia,
Universita' degli Studi di Milano, Via Botticelli, 23,
20133, Milano, Italy
E-mail: diego.gatta@unimi.it
Tel.: +39-02-50315607
Fax: +39-02-50315597

F. Nestola · T. B. Ballaran
Bayerisches Geoinstitut,
Universität Bayreuth, Universität Str. 30,
95447, Bayreuth, Germany

F. Nestola
Crystallography Laboratory,
Department of Geosciences,
Virginia Tech, Blacksburg, VA, 24061, USA

Introduction

Topaz, $Al_2SiO_4(F,OH)_2$, is one of the most important F/OH-bearing silicates, found in different geological environments: as accessory mineral in F-rich granitic rocks, associated to pneumatolithic/hydrothermal events and in UHP units (Pichavant and Manning 1984; Taylor 1992; Taylor and Fallick 1997; Zhang et al. 2002; Alberico et al. 2003). The crystal structure of topaz was first solved by Alston and West (1928) and Pauling (1928). Later, several studies have been devoted to the crystal chemistry/physics of topaz along the solid solution $Al_2SiO_4F_2$–$Al_2SiO_4(OH)_2$ (Ribbe and Gibbs 1971; Ribbe and Rosenberg 1971; Akizuki et al. 1979; Zemann et al. 1979; Parise et al. 1980; Ribbe 1982; Barton 1982; Barton et al. 1982; Northrup et al. 1994; Wunder et al. 1993, 1999; Alberico et al. 2003; Chen and Lager 2005, Chen et al. 2005). For natural topazes, with OH/(OH + F) < 0.5, the crystal structure is described in the *Pbnm* space group, with one H-site (Fig. 1). In contrast, in the crystal structure of the synthetic $Al_2SiO_4(OH)_2$ end-member two non equivalent and partially occupied (50%) H-sites were found and some evidence for a lower symmetry ($Pbn2_1$ space group) has been reported (Northrup et al. 1994; Chen et al. 2005).

The thermal expansion of topaz has first been described by Skinner (1966) by means of in situ X-ray powder diffraction. Later, the thermal and pressure behaviour of a natural topaz ($Al_{2.01}Si_{1.00}O_4F_{1.57}(OH)_{0.43}$) was investigated by Komatsu et al. (2003) by means of in situ X-ray single-crystal diffraction. The HP-lattice parameters have been measured up to about 6.8 GPa. The bulk modulus ($K_{T0} = -V_0(\partial P/\partial V)_{P0}$) has been calculated on the basis of the volume data collected up to 6.2 GPa with a truncated second-order Birch-Murnaghan equation-of-state (II-BM-EoS, Birch 1947), i.e. with the bulk modulus P-derivative ($K' = (\partial K_{T0}/\partial P)_{P0}$) value fixed to 4. The calculated bulk modulus ($K_{T0} = 154(2)$ GPa) significantly differs from the elastic stiffness ($C = 174.3$ GPa) obtained for a natural topaz (whose

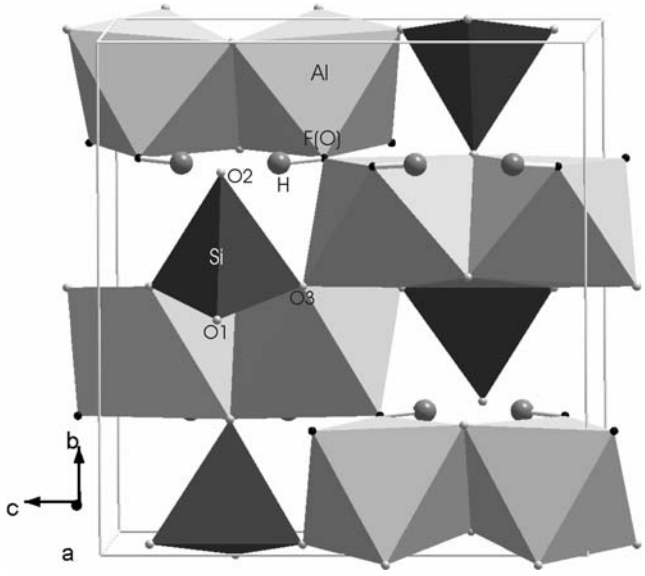

Fig. 1 Clinographic view of the crystal structure of topaz. Site positions from Alberico et al. (2003)

composition was not reported) by Haussühl (1993) by means of ultrasonic resonance experiments. Although the isothermal bulk modulus is always smaller than the elastic stiffness, such large difference may also be due to the fact that the K' value was fixed to 4. Komatsu et al. (2003) provided some structural refinement up to 6.2 GPa. A recent study of Chen and Lager (2005) on the H*P*-behaviour of the synthetic $Al_2SiO_4(OH)_2$ topaz analogue, by means of in situ synchrotron powder diffraction up to 10.2 GPa, determined a bulk modulus value of 145(4) GPa with a II-BM-EoS. However, no H*P*-structural refinement has been provided by Chen and Lager (2005).

In order to determine the K' value of this hard mineral it is necessary to obtain accurate lattice parameters at $P > 6.8$ GPa. The aim of this study is therefore to investigate the H*P* elastic behaviour of a natural F/OH topaz by means of in situ single-crystal diffraction up to pressures in excess of 10 GPa, which will allow a full description of the elastic parameters (i.e. K_{T0}, K', axial bulk moduli and elastic anisotropy). Moreover, structural data at pressure higher than 6 GPa will be collected in order to describe the *P*-induced deformation mechanisms, providing greater insight into the structural evolution with pressure, and an explanation for the elastic anisotropy of (F, OH)-topaz.

Experimental methods

A natural, pale yellow and transparent, gem-quality single-crystal of a pneumatolithic/hydrothermal topaz from Ouro Preto, Minas Gerias, Brasil, was used in this study. Electron microprobe analysis in WDS was performed on a single-crystal (300×200×90 μm) using a fully automated JEOL JXA 8200 microprobe at the Bayerisches Geoinstitut (BGI). Major and minor elements were determined at 15 kV accelerating voltage and 15 nA beam current with a counting time of 20 s. To minimize loss of water and fluorine, due to the electron bombardment, the crystal was mounted in epoxy resin and a defocused beam was used. The standards employed were: orthoclase (Si, TAP), spinel (Al, TAP), periclase (O, LDE1) and fluorite (F, LDE1). The amount of oxygen was measured in order to define the OH content. The chemical formula (obtained by averaging 40 points analyses and on the basis of 2 apfu of Al) is $Al_{2.00}Si_{1.05}O_{4.26}F_{1.75}$, which can be rewritten as $Al_{2.00}Si_{1.05}O_{4.00}(OH_{0.26}F_{1.75})$.

A single-crystal of topaz (160×110×20 μm), optically free of twinning and defect, was used for the H*P*-experiments. Accurate lattice parameters were first measured with the crystal in air (Table 1) by X-ray diffraction on a Huber four-circle diffractometer (non-monochromatized Mo-$K\alpha$ radiation) at the BGI using

Table 1 Unit-cell constants of topaz at different pressures

P (GPa)	*a* (Å)	*b* (Å)	*c* (Å)	*V* (Å^3)
0.0001[a]	4.6629(2)	8.8344(4)	8.3865(3)	345.47(1)
0.0001[b]	4.6627(2)	8.8343(4)	8.3867(2)	345.46(2)
0.41(5)	4.6597(2)	8.8303(3)	8.3799(2)	344.80(2)
1.88(5)	4.6451(2)	8.8108(3)	8.3509(2)	341.78(2)
2.57(5)	4.6378(2)	8.8022(3)	8.3372(2)	340.35(2)
3.14(5)	4.6325(2)	8.7938(3)	8.3254(2)	339.15(2)
3.67(5)	4.6267(2)	8.7872(3)	8.3150(2)	338.05(2)
4.65(5)	4.6179(2)	8.7759(3)	8.2976(2)	336.28(2)
5.16(5)	4.6135(2)	8.7692(3)	8.2887(2)	335.34(2)
5.79(5)	4.6071(2)	8.7614(3)	8.2765(2)	334.08(2)
6.52(5)	4.6009(2)	8.7533(3)	8.2641(2)	332.82(2)
7.41(5)	4.5930(4)	8.7427(5)	8.2488(3)	331.23(3)
8.39(5)	4.5841(4)	8.7308(5)	8.2316(3)	329.45(3)
8.97(5)	4.5795(5)	8.7247(6)	8.2224(4)	328.53(4)
10.01(5)	4.5704(6)	8.7111(7)	8.2038(4)	326.62(4)
10.55(5)	4.5652(5)	8.7046(6)	8.1946(4)	325.64(4)
5.93(5)[c]	4.6054(4)	8.7589(5)	8.2731(3)	333.73(3)
2.41(5)[c]	4.6385(2)	8.8021(3)	8.3382(2)	340.43(2)

Estimated standard deviations are in parenthesis
[a]Data collected with the crystal in air
[b]Data collected with the crystal in the DAC
[c]Data collected during decompression

eight-position centring of 20 Bragg reflections according to the protocol of King and Finger (1979) and Angel et al. (2000). Peak scanning, centring procedure and vector-least-square refinement of the lattice constants were performed by SINGLE04 software (Ralph and Finger 1982; Angel et al. 2000). Following the correlation equation between weight percentage of F (w_F) versus unit-cell constants (calculated on the basis of 33 data available in literature, see Alberico et al. 2003), the a value measured for the crystal in air gives a $w_F = 16.3\%$, equal to a F content of 1.61 apfu, which is slightly lower than the value from the chemical analysis ($w_F = 17.6\%$, 1.75 apfu).

A BGI-diamond anvil cell (DAC), designed by Allan et al. (1996), was used for the H*P*-experiments. Stainless-steel T301 foil, 250 μm thick, pre-indented to a thickness of about 60 μm and with a 250 μm hole obtained by electro-spark erosion, was used as a gasket. The platy crystal of topaz, already studied in air, was loaded into the DAC together with some ruby chips for pressure measurements (Mao et al. 1986). A mixture of methanol:ethanol:water (16:3:1) was used as hydrostatic pressure-transmitting medium (Miletich et al. 2000). Accurate lattice parameters were measured at pressures ranging between 0.0001 and 10.55(5) GPa (Table 1) following the same procedure used for the crystal in air.

Intensity diffraction data were collected on a Xcalibur-Oxford Diffraction diffractometer (Kappa-geometry, graphite-monochromated Mo-$K\alpha$ radiation) at 0.0001 (with the crystal in the DAC), 3.14(5), 5.79(5) and 8.39(5) GPa (Table 2). The reflection conditions were in agreement with the space group *Pbnm*. Integrated intensity data for the structural refinements (corrected for Lorentz-polarisation effects) were obtained using the WinIntegr3.4 program (Angel 2003a, b). The absorption correction due to the crystal and the DAC was performed using the ABSORB5.2 computer program (Burnham 1966; Angel 2002). The crystal structure was then refined with isotropic displacement parameters using the SHELX-97 software (Sheldrick 1997), starting from the atomic coordinates of Alberico et al. (2003). Hydrogen atoms were not included in the structural model. Neutral atomic scattering factors of Si, Al, O and F were used according to the international tables for crystallography (Wilson and Prince 1999). Details of the structural refinements are reported in Tables 2. The refined atomic positions at different pressures are reported in Table 3. Bond distances, polyhedral volumes and other relevant structural parameters are reported in Table 4. Observed and calculated structure factors are deposited and can be obtained from the authors upon request.

Results

Elastic behaviour

The evolution of the unit-cell parameters of topaz between 0.0001 and 10.55(5) GPa is shown in Fig. 2. No phase transition has been observed within the pressure range investigated. Two data points measured during decompression (at 2.41(5) and 5.93(5) GPa) follow the same trend of the data collected during compression (Fig. 2, Table 1). Unit-cell volume data were fitted with a III-BM-EoS. The resulting III-BM-EoS parameters, simultaneously refined using the data weighted by the uncertainties in P and V (Angel 2001), are: $V_0 = 345.57(7)$ Å^3, $K_{T0} = 164(2)$ GPa and $K' = 2.9(4)$. The confidence ellipse at 68.3% level was calculated starting from the variance–covariance matrix of K_{T0} and K' obtained from the least-square procedure (Angel 2000). The ellipse is elongated with a negative slope, indicating a negative correlation of the parameters K_{T0} and K'. The individual values for K_{T0} and K' are 164 ± 4 GPa and 2.9 ± 0.7, respectively. Fitting the cell-volume data with a II-BM-EoS we obtained: $V_0 = 345.69(6)$Å^3, $K_{T0} = 158.2(7)$ GPa ($K' = 4$), but an evident discrepancy was observed between the calculated and the observed cell-volume values at $P > 8$ GPa, signifying that a III-BM-EoS has to be used for the best fit.

A linearized III-BM-EoS (Angel 2000) was used to obtain the axial-EoS parameters, yielding: $a_0 = 4.6634(3)$ Å, $K_{T0}(a) = 152(2)$ GPa [$\beta_a = 1/(3K_{T0}\ (a)) =$

Table 2 Details of data collection and refinements of topaz at different pressures

Pressure (GPa)	0.0001[a]	3.14(5)	5.79(5)	8.39(5)
Radiation	Mo$K\alpha$	Mo$K\alpha$	Mo$K\alpha$	Mo$K\alpha$
2θ range (°)	2–60	2–60	2–60	2–60
Scan type	ω	ω	ω	ω
Scan speed (°/s)	0.05	0.05	0.05	0.05
Scan width (°)	1.20	1.20	1.20	1.20
Detector-sample distance (mm)	135.0	135.0	135.0	135.0
Space group	*Pbnm*	*Pbnm*	*Pbnm*	*Pbnm*
Reflections measured	619	566	567	540
Unique reflection (total)	224	223	213	186
Unique reflection with $F_o > 4\sigma(F_o)$	200	190	184	151
Parameters refined	23	23	23	21
R_{int}	0.060	0.068	0.068	0.112
R_1 (F)	0.045	0.046	0.053	0.062
GooF	1.075	1.168	1.169	1.093

$R_{int} = \Sigma|F^2_{obs} - F^2_{obs}(mean)|/\Sigma[F^2_{obs}]$; $R_1 = \Sigma(|F_{obs}| - |F_{calc}|)/\Sigma|F_{obs}|$

[a]Data collected with the crystal in the DAC without *P*-medium

Table 3 Refined positional and displacement parameters for topaz at different pressures

Site	*x*	*y*	*z*	U_{iso} (Å^2)
Al	0.9047(4)	0.1309(2)	0.0817(1)	0.0053(4)
	0.9047(5)	0.1307(2)	0.0816(2)	0.0053(5)
	0.9064(5)	0.1309(2)	0.0811(2)	0.0055(5)
	0.9069(7)	0.1313(3)	0.0807(2)	0.0041(7)
Si	0.4005(5)	0.9409(2)	0.25	0.0044(5)
	0.4009(6)	0.9407(3)	0.25	0.0041(5)
	0.4023(7)	0.9404(3)	0.25	0.0047(5)
	0.4016(8)	0.9413(4)	0.25	0.0041(7)
O1	0.7963(11)	0.5321(6)	0.25	0.0057(10)
	0.7919(14)	0.5295(7)	0.25	0.0044(11)
	0.7884(14)	0.5295(7)	0.25	0.0046(12)
	0.7882(19)	0.5276(9)	0.25	0.0037(9)
O2	0.4531(10)	0.7559(5)	0.25	0.0035(10)
	0.4471(14)	0.7547(6)	0.25	0.0057(13)
	0.4482(13)	0.7555(6)	0.25	0.0047(13)
	0.4490(19)	0.7546(9)	0.25	0.0037(9)
O3	0.7904(7)	0.0108(4)	0.9069(3)	0.0064(7)
	0.7876(9)	0.0101(5)	0.9080(3)	0.0053(8)
	0.7856(9)	0.0094(5)	0.9092(4)	0.0059(8)
	0.7845(12)	0.0086(7)	0.9094(4)	0.0037(9)
F(O)	0.9006(8)	0.7533(3)	0.0599(3)	0.0117(7)
	0.9021(10)	0.7529(4)	0.0625(4)	0.0129(8)
	0.9046(10)	0.7531(4)	0.0637(3)	0.0110(8)
	0.9075(15)	0.7531(5)	0.0653(4)	0.0112(11)

Estimated standard deviations are in parenthesis. For each atom, values from top to bottom correspond to the refinement at 0.0001, 3.14(5), 5.79(5) and 8.39(5) GPa, respectively. For the refinement at 8.39(5) GPa, the thermal displacement parameters of O1, O2 and O3 have been constrained to have the same value

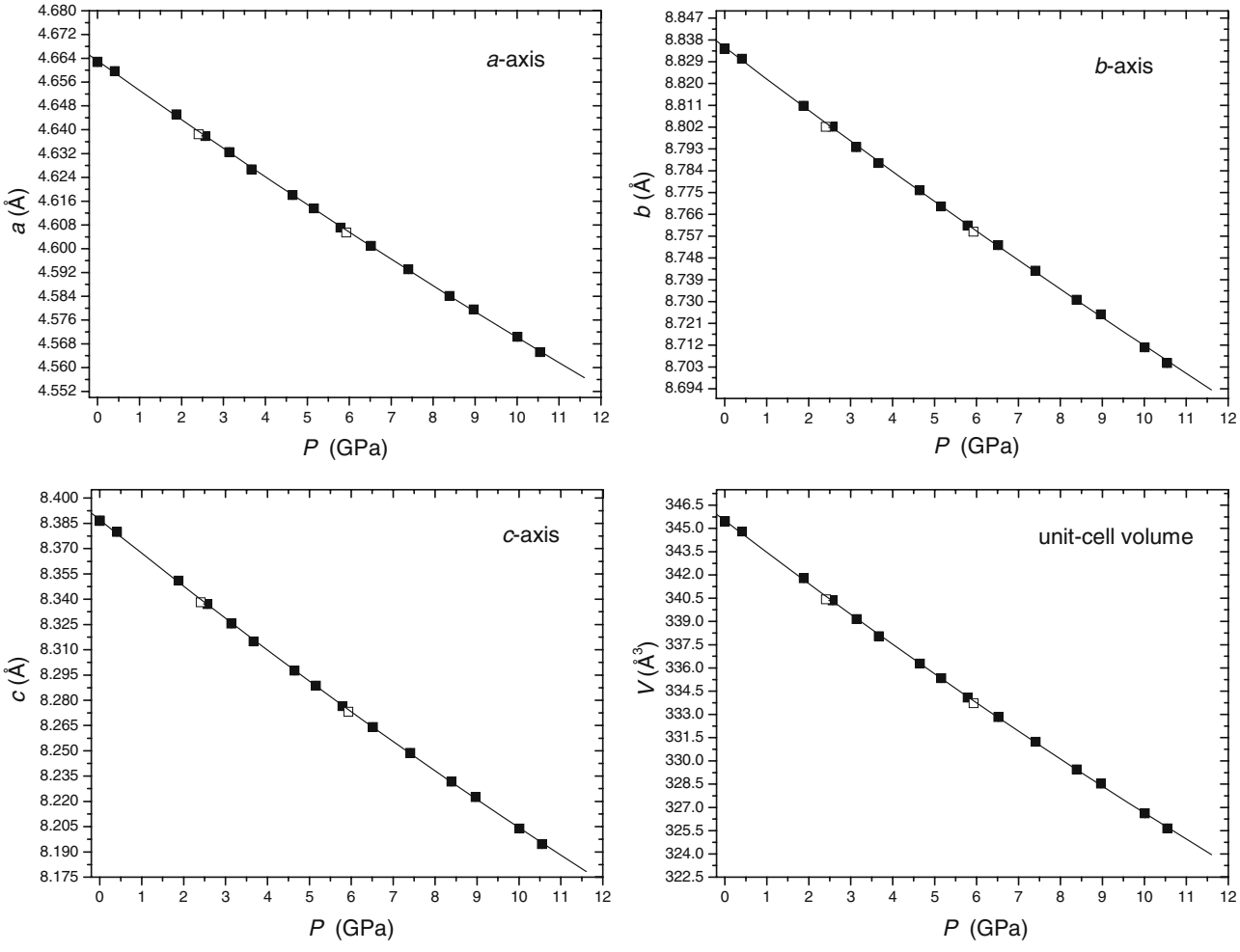

Fig. 2 Variation of the unit-cell parameters with pressure. *Open symbols* represent data collected during decompression. *Solid curves* represent the axial and volume III-BMEoS-fit. *Uncertainties* are smaller than the size of the symbols

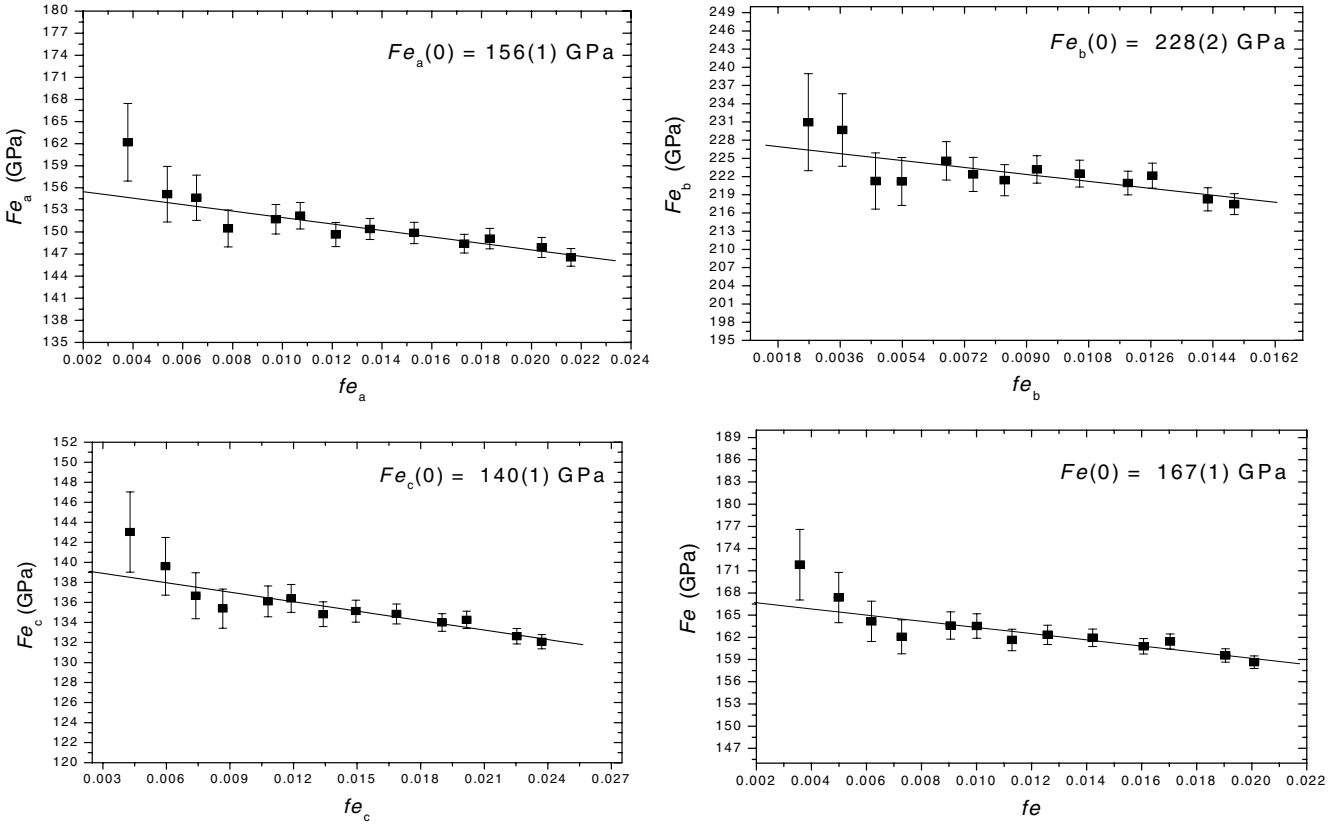

Fig. 3 Axial and volume normalized stress ($F_e = P/[3f_e(1+2f_e)^{5/2}]$) versus eulerian strain ($f_e = [(V_0/V)^{2/3} - 1]/2$) plot for the data points at $P > 0.41$ GPa. The *esds* have been calculated according to Heinz and Jeanloz (1984). The *solid lines* are the weighted linear fit through the data

0.00219(3) GPa^{-1}], $K'(a) = 2.8(4)$ for the *a*-axis; $b_0 = 8.8349(5)$ Å, $K_{T0}(b) = 224(3)$ GPa [$\beta_b = 0.00149$ (2) GPa^{-1}], $K'(b) = 2.6(6)$ for the *b*-axis; $c_0 = 8.3875(7)$ Å, $K_{T0}(c) = 137(2)$ GPa [$\beta_c = 0.00243$ (4) GPa^{-1}], $K'(c) = 2.9(4)$ for the *c*-axis. The elastic anisotropy of topaz appears to be significantly large, with $K_{T0}(a):K_{T0}(b):K_{T0}(c) = 1.11:1.63:1.00$ ($\beta_a:\beta_b:\beta_c = 1.47:1.00:1.63$).

Axial and volume Eulerian finite strain (f_e) and "normalized stress" (F_e) (Angel 2000) have been calculated and the f_e–F_e plots are shown in Fig. 3. The negative slopes obtained from the linear fits of the f_e–F_e plots is in good agreement with the K' values smaller than 4 given by the III-BM-EoS fits.

The magnitudes of the principal Lagrangian unit-strain coefficients (ε_1, ε_2, ε_3) between room pressure and each measured $P > 0.41$ GPa, were calculated with the STRAIN software (Ohashi 1982) (Table 5). The unit-strain ellipsoid is oriented with $\varepsilon_1 || b$, $\varepsilon_2 || a$, $\varepsilon_3 || c$ and $|\varepsilon_3| > |\varepsilon_2| > |\varepsilon_1|$. The magnitude of the strain coefficients slightly decrease with P. At $P - P_0 = 10.55$ GPa, the calculated elastic anisotropy is high, being $\varepsilon_1:\varepsilon_2:\varepsilon_3 = 1.00:1.42:1.56$.

High-pressure structural evolution

Four structural refinements, carried out at 0.0001 (with the crystal in the DAC), 3.14(5), 5.79(5) and 8.39(5) GPa, have been used to give insight into the HP structural evolution of topaz. The Al–O and Si–O bond distances are decreasing as a function of pressure (Table 4) with consequent decreasing of the Al-octahedra and of the Si-tetrahedra volumes (calculated using the IVTON software, Balic Zunic and Vickovic 1996). Although the Si-tetrahedron is less compressible than the Al-octahedron, it is not as stiff as in the Al_2SiO_5 polymorphs sillimanite, andalusite and kyanite (Smyth et al. 2000) or in the garnet structure (Zhang et al. 1998), but it is indeed deforming as suggested by Komatsu et al. (2003). A minor effect of polyhedral tilting is observed between Al-octahedra connected by a F-bridge. The angle Al–F(O)–Al is 143.5(2)° under room condition and decreases to 139.9(5)° at 8.39(5) GPa (Table 4). The main structural deformation mechanism under pressure is therefore represented not by polyhedral tilting but rather by the shortening of the polyhedral bond distances, which imply a reduction of the polyhedral volumes, as expected for a "dense" orthosilicate.

Discussion and conclusions

The precise determination of the unit-cell volume allowed us to refine both the bulk modulus ($K_{T0} = 164(2)$ GPa) and its P-derivative ($K' = 2.9(4)$).

Table 4 Relevant structural parameters of topaz at different pressures

P (Gpa)	0.0001	3.14(5)	5.79(5)	8.39(5)
Al–F(O) (Å)	1.795(4)	1.787(5)	1.793(5)	1.783(5)
Al–F(O) (Å)	1.809(3)	1.809(4)	1.795(4)	1.794(7)
Al–O1 (Å)	1.903(4)	1.889(4)	1.882(4)	1.886(6)
Al–O2 (Å)	1.908(4)	1.899(4)	1.893(4)	1.879(6)
Al–O3 (Å)	1.884(3)	1.867(4)	1.860(4)	1.855(5)
Al–O3 (Å)	1.894(4)	1.888(5)	1.878(5)	1.869(6)
<Al–F/O> (Å)	1.865	1.856	1.850	1.844
$V_{\text{Al-octahedron}}$ (Å^3)	8.575(31)	8.464(36)	8.380(37)	8.306(50)
Si–O1 (Å)	1.625(6)	1.621(7)	1.623(7)	1.608(9)
Si–O2 (Å)	1.650(6)	1.648(7)	1.633(7)	1.643(10)
Si–O3 (×2) (Å)	1.643(3)	1.633(4)	1.635(4)	1.623(5)
<Si–O> (Å)	1.640	1.634	1.631	1.624
$V_{\text{Si-tetrahedron}}$ (Å^3)	2.263(14)	2.236(16)	2.228(17)	2.199(22)
O1–O2 (Å)	2.540(3)	2.541(5)	2.524(4)	2.518(4)
O3–O3 (Å)	2.506(4)	2.494(4)	2.485(5)	2.478(5)
F(O)···F(O) (Å)	3.184(4)	3.111(5)	3.080(5)	3.037(7)
F(O)···O1 (Å)	2.565(3)	2.555(3)	2.548(4)	2.545(7)
F(O)···O1 (Å)	3.070(4)	3.021(4)	3.004(5)	2.974(5)
F(O)···O2 (Å)	2.609(3)	2.602(3)	2.601(4)	2.599(5)
F(O)···O2 (Å)	3.026(4)	2.963(5)	2.938(4)	2.909(9)
F(O)···O3 (Å)	2.545(3)	2.540(5)	2.532(5)	2.501(6)
F(O)···O3 (Å)	2.648(4)	2.638(4)	2.636(4)	2.633(7)
F(O)···O3 (Å)	2.658(4)	2.650(4)	2.640(5)	2.639(9)
F(O)···O3 (Å)	2.967(3)	2.929(5)	2.900(4)	2.871(6)
Al–F(O)–Al (°)	143.5(2)	142.2(2)	141.1(2)	139.9(5)

Estimated standard deviations are in parenthesis. The bulk modulus of the Al-octahedron and the Si-tetrahedron calculated with a linear regression through the data point (as inverse of the compressibility coefficients) are 270(8) and 328(42), respectively

The bulk modulus value obtained in this study is in between the K_{T0} value obtained by Komatsu et al. (2003) (K_{T0} = 154(2) GPa) and the mean elastic stiffness (C = 174.3 GPa) reported by Haussül (1993) by means of ultrasonic resonance data. The difference between the K_{T0} of this study and that of Komatsu et al. (2003) may be due to the different K' used, since Komatsu et al. (2003) implied a K' value of 4 whereas from our data K' is clearly less than 4. Also the differences in K_{T0} values may be due to the different composition of the topaz samples used in the different studies, as the fluorine content of the sample used by Komatsu et al. (2003) (1.57 apfu) was slightly less than that of our sample. Considering the results of this study and those of Komatsu et al. (2003) and Chen and Lager (2005) we observe a relationship between the F-content and the bulk modulus: the higher the amount of fluorine, the higher is the bulk modulus value. A similar effect was observed in (F, OH)-substituted humites (Ross and Crichton 2001; Friedrich et al 2002).

The anisotropic behaviour of topaz obtained in this study is in general agreement with the results reported by of Komatsu et al. (2003), who provided the axial compressibility coefficient up to 6.2 GPa on the basis of a linear regression trough the data point (β_a:β_b:β_c = 1.42:1.00:1.58).

The orientation of the strain ellipsoid and the magnitude of the principal unit-strain coefficients show that under pressure the maximum and the minimum shortening of the topaz structure are along [001] and [010] respectively. The reasons of the observed anisotropic compression can be intuitively deduced from the topo-

Table 5 Magnitude of the principal Lagrangian unit-strain coefficients (between room pressure and P > 0.41 GPa) and orientation of the unit-strain ellipsoid at high-pressure

$P-P_0$ (GPa)	$\|\varepsilon 1\|$ (GPa^{-1})	$\|\varepsilon 2\|$ (GPa^{-1})	$\|\varepsilon 3\|$ (GPa^{-1})
1.88	0.00142(8)	0.00201(9)	0.00226(8)
2.57	0.00142(8)	0.00208(10)	0.00230(8)
3.14	0.00146(8)	0.00207(9)	0.00232(8)
3.67	0.00146(8)	0.00211(9)	0.00233(9)
4.65	0.00142(8)	0.00207(9)	0.00229(8)
5.16	0.00143(8)	0.00204(10)	0.00226(8)
5.79	0.00143(8)	0.00206(10)	0.00227(8)
6.52	0.00141(9)	0.00203(11)	0.00224(8)
7.41	0.00140(10)	0.00202(10)	0.00222(9)
8.39	0.00140(9)	0.00201(11)	0.00220(9)
8.97	0.00138(10)	0.00199(11)	0.00218(9)
10.01	0.00139(10)	0.00198(11)	0.00218(10)
10.55	0.00139(12)	0.00198(12)	0.00217(11)

Estimated standard deviations are in parenthesis. $\varepsilon_1 \| b$, $\varepsilon_2 \| a$, $\varepsilon_3 \| c$

logical configuration of polyhedra and their inter-polyhedral asset. Given that the Si-tetrahedra are the less compressible polyhedra, we can expect that the effect of pressure will be accommodated mostly by the Al-octahedra and the voids. Figure 4 presents the view of the crystal structure of topaz down the *a*-axis and the correlated unit-strain ellipsoid. It can be noticed that along the *c*-axis tetrahedra and octahedra are alternated giving rise to ''weak zones'' (i.e. ''tetrahedra-free zones'' in light-grey overlaying the crystal structure in Fig. 4) which are more compressible. The ''tetrahedra-free zone'' concept was already used in order to explain the {001}-cleavage observed for natural topaz crystal (Ribbe and Gibbs 1971). The compressibility along [001] is basically due to the reduction of the O3–O3 distance, which represents one edge shared by two Al-octahedra in the ''weak zone'' (Fig. 4, Table 4), and to the bond distance Al–O3, with a reduction of 1.12 and 1.54% between 0.0001 and 8.39(5) GPa, respectively. Within the same *P*-range, the distance O2–O1, which reflects the contraction along [010] (Fig. 4), shows a reduction of only 0.87% (Table 4). The anisotropic decrease of the bond distances with *P* causes a distortion of the octahedra.

The bulk moduli of the SiO_4 tetrahedron (328(42) GPa) and AlO_4F_2 octahedron (270(8) GPa, Table 3) determined in this study are in good agreement with those reported by Komatsu et al. (2003) (324(76) and 251(19) GPa, respectively) within the *esds*. In addition, the AlO_4F_2 octahedra appear to be more compressible than expected in comparison to the bulk modulus-volume relationship of the AlO_6 octahedra in the Al_2SiO_5 polymorphs (Komatsu et al. 2003; Yang et al. 1997).

Due to the impossibility of determining the hydrogen positions in the H*P* structural refinements, the topological configuration of the OH group and the role played by the H-bonds under pressure on the structural evolution has not been characterised. Natural topaz possess weak hydrogen bonding at room pressure with the O1 and O2 sites as possible hydrogen bond acceptors (Belokoneva et al. 1993). The F(O)···O1 and F(O)···O2 distances decrease with pressure, moreover the distance F(O)···F(O) decreases from 3.184(4) Å at 0.0001 GPa to 3.037(7)Å at 8.39(5) GPa, suggesting a strengthening of H-bonding. However H*P* Raman and IR experiments performed by Bradbury and Williams (2003) and Komatsu et al. (2005) suggest that the H-bonds in natural F/OH-topazes does not change with increasing pressure. As stated by Komatsu et al. (2005), the strength of the H-bond is also controlled by the F(O)–H···O angle, since such angular value influences the degree of H(*s*)–O(*2p*) orbital overlap of the bond (Hofmeister et al. 1999; Kagi et al. 2003). Therefore, a neutron diffraction study at H*P* is necessary in order to locate the H-sites under pressure and to provide a structural model for the O–H vibrational modes.

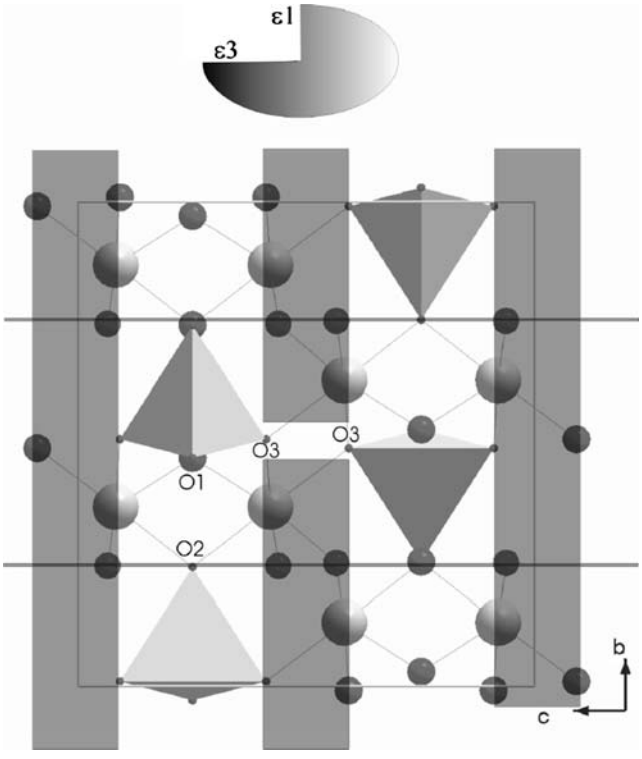

Fig. 4 Oriented unit-strain ellipsoid and crystal structure of topaz viewed down [100]. Tetrahedral sites are shown as *closed-faces polyhedra*; octahedral sites are represented as *balls and sticks*. The ''weak zones'' (see text) are represented in *light-grey* overlying the crystal structure

Acknowledgements The authors are indebted with St. Putignano, the Italian collector who provided the natural sample of topaz used in this study. This work was financially supported by the Sofia Kovalevskaja Award to T. Boffa Ballaran and the A. von Humboldt Foundation to F. Nestola. M. Rieder and P. Dera are thanked for their helpful suggestions.

References

Akizuki M, Hampar MS, Zussman J (1979) An explanation of anomalous optical properties of topaz. Min Mag 43:237–241

Alberico A, Ferrando S, Ivaldi G, Ferraris G (2003) X-ray single-crystal structure refinement of an OH-rich topaz from Sulu UHP terrane (Eastern China)—structural foundation of the correlation between cell parameters and fluorine content. Eur J Mineral 15:875–881

Alston NA, West J (1928) The structure of topaz. Proc R Soc A121:358–367

Allan DR, Miletich R, Angel RJ (1996) A diamond-anvil cell for single-crystal X-Ray diffraction studies to pressures in excess of 10 GPa. Rev Sci Instrum 67:840–842

Angel RJ (2000) Equation of state. In: Hazen RM, Downs RT (eds) High-temperature and high-pressure crystal chemistry. Reviews in mineralogy and geochemistry, vol 41. Mineralogical Society of America and Geochemical Society, Washington, pp 35–59

Angel RJ (2001) EOS-FIT V6.0. Computer program. Crystallography Laboratory, Department of Geological Sciences, Virginia Tech, Blacksburg, USA

Angel RJ (2002) ABSORB V5.2. Computer program. Crystallography Laboratory, Department of Geological Sciences, Virginia Tech, Blacksburg, USA

Angel RJ (2003a) Automated profile analysis for single-crystal diffraction data. J Appl Crystallogr 36:295–300

Angel RJ (2003b) WIN-INTEGRSTP V3.4. Computer program. Crystallography Laboratory, Department of Geological Sciences, Virginia Tech, Blacksburg, USA

Angel RJ, Downs RT, Finger LW (2000) High-temperature–high-pressure diffractometry. In: Hazen RM, Downs RT (eds) High-temperature and high-pressure crystal chemistry. Reviews in mineralogy and geochemistry, vol 41, Mineralogical Society of America and Geochemical Society, Washington, pp 559–596

Balic Zunic T, Vickovic I (1996) IVTON—a program for the calculation of geometrical aspects of crystal structures and some crystal chemical applications. J Appl Crystallogr 29:305–306

Barton MD (1982) The thermodynamic properties of topaz solid solution and some petrological applications. Am Mineral 67:956–974

Barton MD, Haselton HT Jr, Hemingway BS, Kleppa OJ, Robie RA (1982) The thermodynamic properties of fluor-topaz. Am Mineral 67:350–355

Belakoneva EL, Smirnitskaya YY, Tsirel'son VG (1993) Electron density distribution in topaz $Al_2[SiO_4](F,OH)_2$ as determination from high-precision X-ray diffraction data. Russ J Inorg Chem 38–8:1252–1256

Birch F (1947) Finite elastic strain of cubic crystal. Phys Rev 71:809–824

Bradbury SE, Williams Q (2003) Contrasting bonding behavior of two hydroxyl-bearing metamorphic minerals under pressure: Clinozoisite and topaz. Am Mineral 88:1460–1470

Burnham CW (1966) Computation of absorption corrections and the significance of end effects. Am Mineral 51:159–167

Chen J, Lager G (2005) High-pressure infrared and powder X-ray study of topaz-OH: Comparison with hydrous magnesium silicate (humite). COMPRES 4th annual meeting, Mohonk Mountain House, New Paltz, NY, 16–19 June 2005

Chen J, Lager GA, Kunz M, Hansen T, Ulmer P (2005) A Rietveld refinement using neutron powder diffraction data of a fully deuterated topaz, $Al_2SiO_4(OD)_2$. Acta Cryst E61:i253–i255

Friedrich A, Lager GA, Ulmer P, Kunz M, Marshall WG (2002) High-pressure single-crystal X-ray and powder neutron study of F, OH/OD-chondrodite: compressibility, structure and hydrogen bonding. Am Mineral 87:931–939

Haussühl S (1993) Thermoelastic properties of beryl, topaz, diaspore, sanidine and periclase. Z Kristallogr 204:67–76

Heinz DL, Jeanloz R (1984) The equation of state of the gold calibration standard. J Appl Phys 55:885–893

Hofmeister AM, Cynn H, Burnley PC, Meade C (1999) Vibrational spectra of dense, hydrous magnesium silicates at high pressure: importance of the H bond angle. Am Mineral 84:454–464

Kagi H, Nagai T, Loveday JS, Wada C, Parise JB (2003) Pressure-induced phase transformation of kalicinite ($KHCO_3$) at 2.8 GPa and local structural changes around hydrogen atoms. Am Mineral 88:1446–1451

King HE, Finger LW (1979) Diffracted beam crystal centering and its application to high-pressure crystallography. J Appl Crystallogr 12:374–378

Komatsu K, Kuribayashi T, Kudoh Y (2003) Effect of temperature and pressure on the crystal structure of topaz, $Al_2SiO_4(OH, F)_2$. J Mineral Petrol Sci 98:167–180

Komatsu K, Kagi H, Okada T, Kuribayashi T, Parise JB, Kudoh Y (2005) Pressure dependence of the OH-stretching mode in F-rich natural topaz and topaz-OH. Am Mineral 90:266–270

Mao HK, Xu J, Bell PM (1986) Calibration of the ruby pressure gauge to 800 kbar under quasi-hydrostatic conditions. J Geophys Res 91:4673–4676

Miletich R, Allan DR, Kush WF (2000) High-pressure single-crystal techniques. In: Hazen RM, Downs RT (eds) High-temperature and high-pressure crystal chemistry. Reviews in mineralogy and geochemistry, vol 41, Mineralogical Society of America and Geochemical Society, Washington, pp 445–519

Northrup PA, Leinenweber K, Parise JP (1994) The location of H in the high-pressure synthetic $Al_2SiO_4(OH)_2$ topaz analogue. Am Mineral 79:401–404

Ohashi Y (1982) STRAIN: A program to calculate the strain tensor from two sets of unit-cell parameters. In: Hazen RM, Finger LW (eds) Comparative Crystal Chemistry. Wiley, New York, pp 92–102

Parise JB, Cuff C, Moore FH (1980) A neutron diffraction study of topaz: evidence for lower symmetry. Min Mag 43:943–944

Pauling L (1928) The crystal structure of topaz. Proc Natl Acad Sci USA 14:603–606

Pichavant M, Manning D (1984) Petrogenesis of tourmaline granites and topaz granites: the contribution of experimental data. Phys Earth Plan Int 35:31–50

Ralph RL, Finger LW (1982) A computer program for refinement of crystal orientation matrix and lattice constants from diffractometer data with lattice symmetry constraints. J Appl Crystallogr 15:537–539

Ribbe PH (1982) Topaz. In: Ribbe PH (ed) Orthosilicates, 2nd edn, vol 5. Reviews in mineralogy, Mineralogical Society of America, Washington, pp 215–230

Ribbe PH, Gibbs GV (1971) The crystal structure of topaz and its relation to physical properties. Am Mineral 56:24–30

Ribbe PH, Rosenberg PE (1971) Optical and X-ray determinative methods for fluorine in topaz. Am Mineral 57:168–187

Ross NL, Crichton WA (2001) Compression of hydroxy-clinohumite ($Mg_9Si_4O_{16}(OH)_2$) and hydroxy-chondrodite ($Mg_5Si_2O_8(OH)_2$). Am Mineral 86:990–996

Sheldrick GM (1997) SHELX-97 programs for crystal structure determination and refinement. Institut für Anorg Chemie University of Göttingen, Germany

Skinner BJ (1966) Thermal expansion. In: Clark SP (ed) Handbook of physical constants. Geol Soc Am Mem, pp 75–95

Smyth JR, Jacobsen SD, Hazen RM (2000) Comparative crystal chemistry of orthosilicate minerals. In: Hazen RM, Downs RT (eds) High-temperature and high-pressure crystal chemistry. Reviews in mineralogy and geochemistry, vol 41, Mineralogical Society of America and Geochemical Society, Washington, pp 187–209

Taylor RP (1992) Petrological and geochemical characteristics of the Pleasant Ridge zinnwaldite-topaz granite, southern New Brunswick, and comparisons with other topaz-bearing felsic rocks. Can Mineral 30:895–921

Taylor RP, Fallick AE (1997) The evolution of fluorine-rich felsic magmas: source dichotomy, magmatic convergence and the origins of topaz granite. Terra Nova 9:105–108

Wilson AJC, Prince E (eds) (1999) International tables for X-ray crystallography, Mathematical, physical and chemical tables, 2nd edn, vol C. Kluwer, Dordrecht

Wunder B, Rubie DC, Ross CR, Medenbach O, Seifert F, Schreyer W (1993) Synthesis, stability, and properties of $Al_2SiO_4(OH)_2$: a fully hydrated analogue of topaz. Am Mineral 78:285–297

Wunder B, Andrut M, Wirth R (1999) High-pressure synthesis and properties of OH-rich topaz. Eur J Mineral 11:803–813

Yang H, Downs RT, Finger LW, Hazen RM, Prewitt CT (1997) Compressibility and crystal structure of kyanite, Al_2SiO_5, at high pressure. Am Mineral 82:467–474

Zhang L, Ahsbahs H, Kutoglu A (1998) Hydrostatic compression and crystal structure of pyrope to 33 GPa. Phys Chem Miner 25: 301–307

Zhang RY, Liou JG, Shu JF (2002) Hydroxyl-rich topaz in high-pressure and ultrahigh-pressure kyanite quartzites, with retrograde woodhouseite, from the Sulu terrane, eastern China. Am Mineral 87:445–453

Zemann RY, Zobetz E, Heger G, Vollenke H (1979) Structurbestigmmung eines OH-reichen Topases. Österreichische Akad Wiss Mathem Naturwiss Klasse 116:145–147